Catalysis Today 142 (2009) 175–180

Contents lists available at ScienceDirect

Catalysis Today

journal homepage: www.elsevier.com/locate/cattod

Sb-V-O_x catalysts—Role of chemical composition of MCM-41 supports in physicochemical properties

H. Golinska [a], P. Decyk [a,*], M. Ziolek [a], J. Kujawa [a], E. Filipek [b]

[a] Adam Mickiewicz University, Faculty of Chemistry, Grunwaldzka 6, 60-780 Poznań, Poland
[b] Department of Inorganic and Analytical Chemistry, Szczecin University of Technology al. Piastow 42, 71-065, Szczecin. Poland

ARTICLE INFO

Article history:
Available online 17 December 2008

Keywords:
$SbVO_x$ on MCM-41, AlMCM-41, NbMCM-41
Acid–base characterisation
Methanol hydrosulphurisation

ABSTRACT

$SbVO_x$ binary oxides were loaded on MCM-41 matrices of various chemical compositions: silicate (MCM-41), Nb-silicate (NbMCM-41), and Al-silicate (AlMCM-41). Vanadium and antimony were introduced by the post synthesis wetness impregnation carried out step by step (first V next Sb). The materials were characterised by N_2 adsorption/desorption, XRD, UV–vis, ESR, H_2-TPR, FT-IR combined with pyridine adsorption, and test reaction–hydrosulphurisation of methanol. $SbVO_x$ dispersion was much higher when the support contained transition metal (NbMCM-41). Tetrahedrally coordinated vanadium(IV) species were deduced on all prepared samples from UV–vis spectra and were the only registered species on SbV/NbMCM-41 and SbV/AlMCM-41, whereas octahedrally ones were also present on SbV/MCM-41 and SbV/SiO_2. In bulk $SbVO_x$ octahedral coordination dominated. The chemical composition of mesoporous support determined acidic–basic properties of $SbVO_x$ catalysts and influenced the activity and selectivity in methanol hydrosulphurisation. The presence of Lewis acid–base pairs in the SbV/AlMCM-41 and SbV/NbMCM-41 catalysts strongly activated thiol formation in the reaction between methanol and hydrogen sulphide, whereas bulk binary oxides and $SbVO_x$ loaded on silicate MCM-41 were less active and exhibited different selectivity.

1. Introduction

Vanadium–antimony oxides are well known as catalysts for selective oxidation and ammoxidation reactions [1,2]. The activity and selectivity of catalysts in these processes are greatly dependent on the loading (Sb:V atomic ratio), method of preparation, gas phase composition during the thermal treatment, and the nature of the support [3]. Moreover, the role of the nature of antimony complex used during the preparation of the catalysts was stressed [4,5]. Sb-V-O_x catalysts with an excess of V are highly active and selective for propane oxidative dehydrogenation while an excess of Sb affords Sb-V-O_x catalyst more efficient for propane ammoxidation [6,7].

In this work mesoporous materials of MCM-41 type with various chemical composition have been applied as supports for vanadium and antimony which were loaded on the matrix step by step, first vanadium next antimony sources. Mesoporous materials seems to be attractive supports for binary oxides because of their ordered structure. Such materials can be functionalised by various methods. Post synthesis modification of mesoporous molecular sieves via impregnation often leads to the introduction of part of the metal into the framework. Many reports concern the doping of MCM-41 with vanadium with various methods [8–21]. According to our knowledge there is no literature data concerning binary oxide, Sb-V-O_x, loaded on mesoporous molecular sieves with various chemical composition. Chemical composition of the support determines the strength of interaction of the active species with the matrix and leads to various crystalline structures and various catalytic activities. Guerrero-Perez et al. [6] studied the catalysts formed by $SbVO_x$ supported on niobia and alumina. Various structures of $SbVO_x$ were formed depending on the support and niobia appeared to be more attractive support for the catalysts applied in ammoxidation of propane. Alumina interacts weakly with the supported oxides while niobia forms new phases through solid state reaction with the supported oxides during catalytic operation.

We wished to form binary oxides (possible $SbVO_5$ structure) with the excess of vanadium on the surface of silicate, alumino-silicate and niobosilicate MCM-41 materials. The role of SiMCM-41, AlMCM-41 and NbMCM-41 supports on the physicochemical properties of Sb-V-O_x phase was examined in this work. Moreover, we compared these properties with those of bulk binary $SbVO_x$ oxides with various compositions. The idea of the generation of $SbVO_5$ structure on the surface of ordered mesoporous materials

* Corresponding author.
E-mail address: piotrd@amu.edu.pl (P. Decyk).

0920-5861/$ – see front matter © 2008 Published by Elsevier B.V.
doi:10.1016/j.cattod.2008.10.044

was dictated by the lack of papers describing the activity of such forms. Following the successful synthesis of this compound in the bulk form [22] we have applied the similar procedure for the formation of binary oxides on mesoporous supports expecting the creation of activity in sulphurisation process.

2. Experimental

MCM-41 was synthesized following the procedure reported originally by Kresge et al. [23]. The hydrothermal synthesis of NbMCM-41 and AlMCM-41 materials (with Si/Nb = 64 and Si/Al = 32) were performed according to the commonly used procedure described elsewhere [24]. Sodium silicate (27% SiO_2 in 14% NaOH; Aldrich), ammonium niobate(V) oxalate hydrate ($C_4H_4NNbO_9$ - CBMM) and aluminium sulphate (Aldrich) were used as silicon and metal sources, whereas cetyltrimethylammonium chloride (25 wt.% in water; Aldrich) was applied as a template. These mesoporous molecular sieves with various compositions (SiMCM-41; AlMCM-41-32, Si/Al = 32; NbMCM-41-64, Si/Nb = 64) and SiO_2 (Degussa AG) were modified by wetness impregnation with vanadium or/and antimony sources – NH_4VO_3 (BDH Chemicals Ltd.) dissolved in H_2O and $(CH_3COO)_3Sb$ (Aldrich) dissolved in methanol, respectively. The amounts of both solutions were accounted for 5 wt.% of V and Sb loading giving rise to V:Sb = 2.4:1 atomic ratio. The samples containing both metal species (V and Sb) were prepared step by step. First, the impregnation with NH_4VO_3 solution was performed.

The outgased calcined mesoporous material (353 K, 1 h in evaporator) was filled in with the appropriate amount of an aqueous solution of V precursor and placed in an evaporator flask, where the catalyst was rotated and heated at 353 K for ca 12 h. After such drying the impregnation with $(CH_3COO)_3Sb$ was carried out. Finally the catalysts were dried at 353 K for 12 h and calcined in air at 923 K for 96 h. The acronym, of such obtained samples is SbV/MCM-41, whereas that after impregnation with vanadium source—V/MCM-41.

The prepared materials were characterized by XRD (D8 Advance, Bruker diffractometer, CuKα radiation (λ = 0.154 nm). The surface area and pore volume of the MCM-41 materials were estimated by nitrogen adsorption at 77 K using the conventional technique on a Micromeritics 2010 apparatus. Prior to the adsorption measurements, the samples were degassed in vacuum at 573 K for 2 h.

UV–vis spectra were registered using a Varian-Cary 300 Scan UV–visible spectrophotometer. Catalyst powders were placed into the cell equipped with a quartz window. The Kubelka–Munk function ($F(R)$) was used to convert reflectance measurements into equivalent absorption spectra using the reflectance of SPECTRALON as a reference.

The electron spin resonance (ESR) investigations were carried out at 77 K using RADIOPAN SE/X 2547 spectrometer. A cavity operating at a frequency of 8.9 GHz (X-band) with 100 kHz field modulation was used.

The temperature programmed reduction (H_2-TPR) of the samples was performed using H_2/Ar (10 vol.%) as reducing agent (flow rate = 70 $cm^3\ min^{-1}$). The sample (0.03 g) was filled in a quartz tube, treated in a flow of helium at 673 K for 2 h and cooled to room temperature. Then it was heated at a rate of 10 K min^{-1} up to 1273 K under the reducing mixture. Hydrogen consumption was measured by a thermal conductivity detector.

Infrared spectra were recorded with a Bruker Vector 22 FT-IR spectrometer using an in situ cell. Samples were pressed under low pressure into a thin wafer and placed inside the cell. Catalysts were evacuated at 673 K during 2 h and pyridine (PY) was then admitted at 373 K. After saturation with PY the samples were degassed at 373, 423, 473, 523 K in vacuum for 30 min. Spectra were recorded at room temperature in the range from 4000 to 400 cm^{-1}. The spectrum without any sample (“background spectrum”) was subtracted from all recorded spectra. The IR spectra of the activated samples (after evacuation at 673 K) were subtracted from those recorded after the adsorption of PY followed by various treatments. The reported spectra are the results of this subtraction and are calculated per 10 mg of the samples.

Methanol hydrosulphurisation was carried out in a fixed-bed flow reactor. 0.02 g of the catalyst, with a size fraction of 0.5 mm < Ø < 1 mm was placed in the reactor. The samples were activated in helium flow (40 $cm^3\ min^{-1}$) at 723 K for 2 h. Next the temperature was brought to 623 K. The reactant gas mixture of CH_3OH/H_2S/He, molar ratio of ∼5/1/34, was used with a total flow rate of 40 $cm^3\ min^{-1}$. The reactor effluent was analysed using an on line gas chromatograph (SRI 8610 GAS) with FID and FPD detectors.

3. Results and discussion

Texture parameters of the selected samples (the supports and materials containing Sb and V) based on nitrogen adsorption isotherms are shown in Table 1.

Surface area, pore volume and diameter significantly decreased after impregnation with vanadium source. After the next impregnation with antimony the further decrease of these parameters is significant on silicate MCM-41 support. The growth of wall thickness of the impregnated materials suggests the partially incorporation of metals into the framework of walls.

Fig. 1 shows the small-angle XRD patterns which are characteristic of the mesostructured materials with ordered hexagonal arrangement (*p6mm* symmetry). They are characterised by a single Bragg peak (1 0 0) at $2\theta \sim 2^\circ$ and up to three peaks in the region of $2\theta \sim 3$–8°. The latter are not very well resolved, especially for SbV/MCM-41 sample, showing a partially disordering of the hexagonal structure in the long-range.

The idea of the MCM-41 impregnation with vanadium and antimony sources was to locate Sb-V-O_x species on the high surface area of mesoporous materials with various composition. We expected the different metal oxides–support interaction depending on the chemical composition of the support and due to that

Table 1
Texture/structure parameters from nitrogen adsorption isotherms and number of BrØnsted acid sites (BAS) calculated for 10 mg of the samples from FT-IR spectra after pyridine adsorption (∼1550 cm^{-1}; extinction coefficient 1.8 μmol^{-1} [27]).

Catalyst	Surface area ($m^2\ g^{-1}$)	Pore volume BJH ($cm^3\ g^{-1}$)	Mesopore diameter PSD (nm)	Wall thickness (nm)	Number of BAS × 10^{17}
MCM-41	966	1.4	2.8	1.7	0
V/MCM-41	631	0.7	2.2	1.9	0
SbV/MCM-41	483	0.6	2.1	2.3	0
AlMCM-41	950	1.2	2.8	1.8	107
V/AlMCM-41	597	0.7	2.6	1.8	87
SbV/AlMCM-41	671	0.7	2.2	2.0	26
NbMCM-41	1098	1.8	2.8	1.8	0
V/NbMCM-41	886	1.0	2.2	2.1	0
SbV/NbMCM-41	885	1.0	2.2	1.8	0

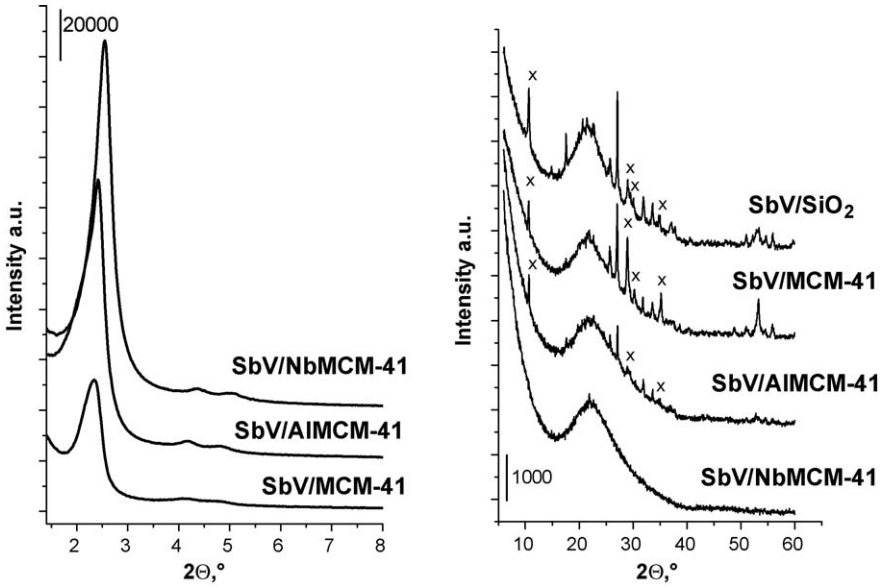

Fig. 1. Small-angle XRD patterns of mesoporous materials and wide-angle dyfractograms of $SbVO_x$ loaded on various matrices.

various catalytic properties of the final materials. The presence of bimetallic oxides was estimated on the basis of wide-angle XRD patterns (Fig. 1). It is characteristic that well visible forms of Sb-V-O_x crystalline bimetallic oxides (one identified as $SbVO_5$, peaks marked by "*x*" [22] and the other peaks suggest the rutile $SbVO_{4.5}$ phase) were detected on silica and silicate MCM-41, whereas on AlMCM-41 they were less visible and on NbMCM-41 were not detected. The lack of XRD reflections can be caused by the small particles of well dispersed crystallites (Sb-V-O_x species) or the absence of crystalline forms. Vanadium species introduced in the first step of modification stronger interact with NbMCM-41 support than with the silicate one. It was evidenced by the results of H_2-TPR (Fig. 2) indicating the higher reduction temperature of vanadium species located on niobiosilicate mesoporous material. Vanadium species stronger hold on the surface does not migrate too easy during calcination performed after the next impregnation with Sb source and therefore does not agglomerate to bigger crystallites possible for detection in XRD technique. It could be a reason of the lack of peaks in XRD patterns and suggests the high dispersion of Sb-V-O_x phase on NbMCM-41.

Vanadium species in the prepared samples has been estimated by UV–vis and ESR spectroscopic study (Figs. 3 and 4). According to the literature [14–16,18], the UV–vis region examined is associated with oxygen to vanadium electron transfer, mainly characteristic of V(V) ions. The lower energy charge transfer (LCT) band for octahedral coordination is falling in the 333–500 nm region. In tetrahedral vanadium(V) compounds, in contrast, the LCT band was found at ~333 nm and the second charge transfer (CT) transition band appears at ~278 nm. The LCT transition for V(IV) falls at higher frequencies in the 286–250 nm region. In the visible region the d–d transitions of VO^{2+} ions could be observed (near 600 and 770 nm). Since the d–d transitions of vanadyl VO^{2+} ions are generally 10–30 times weaker than those of charge transfer transitions [14], such absorption is apparently undetected by diffuse reflectance UV–vis. It is worthy of notice that the second coordination sphere (like in the siliceous mesoporous matrix or in

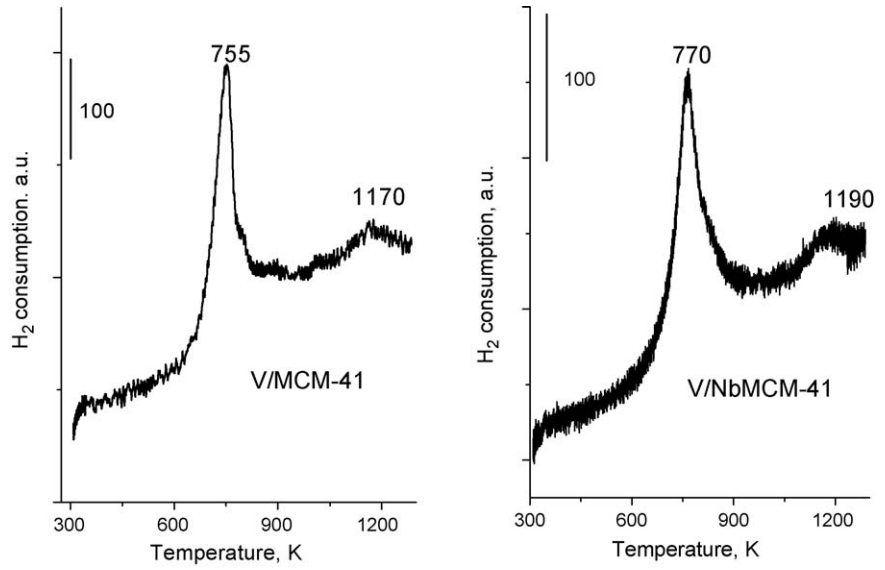

Fig. 2. H_2-TPR results.

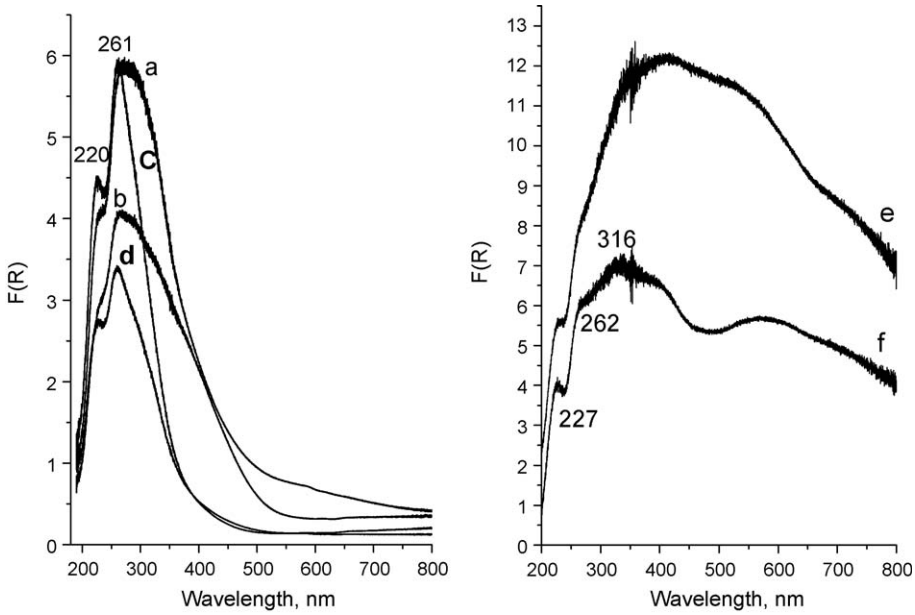

Fig. 3. UV–vis spectra of: (a) SbV/MCM-41; (b) SbV/SiO_2; (c) SbV/NbMCM-41; (d) SbV/AlMCM-41; (e) $Sb_{0.92}{}^{5+}V_{0.64}{}^{4+}V_{0.28}{}^{3+}{}_{\cdot 0.16}O_4$ and (f) $Sb^{5+}V^{4+}O_{4.5}$.

binary Sb-V-O_x oxide) for vanadium–oxygen complex can change slightly the above described positions of UV–vis bands.

Fig. 3 exhibits the UV–vis spectra of bulk $SbVO_x$ compounds ($Sb_{0.92}{}^{5+}V_{0.64}{}^{4+}V_{0.28}{}^{3+}{}_{\cdot 0.16}O_4$ and $Sb^{5+}V^{4+}O_{4.5}$) prepared and described in [22,25,26] and $SbVO_x$ loaded on supports. It is well evidenced that bulk compounds with various compositions possess octahedrally coordinated vanadium(IV) species, whereas $SbVO_x$ loaded on the supports mainly exhibit tetrahedrally coordinated species characterized by the bands at 220 and ~260 nm. However, the difference in UV–vis spectra depending on the nature of the support is well visible. $SbVO_x$ loaded on silica and silicate MCM-41 materials gives rise to the tails in the spectra covering the regions of octahedrally coordinated species like in the bulk binary oxides. This behaviour well correlates with the observation of $SbVO_x$ crystalline phases in XRD patterns, mainly of SbV/SiO_2 and SbV/MCM-41 samples.

ESR spectra allow us to identify VO^{2+} ions in some of the materials studied (Fig. 4, Table 2). Various vanadium(IV) species can be detected by the ESR technique. V(IV) clusters lead to a broad signal owing to significant dipolar interactions which were found e.g. in VMCM-41 samples with a high vanadium content, where vanadium was introduced in one pot synthesis [14,18]. The isolated V(IV) species, mainly in the form of oxovanadium VO^{2+} ions, exhibit a hyperfine structure (ESR signal splits eightfold) derived from the interaction of free electrons ($3d^1$) with the magnetic nuclear moment of ^{51}V ($I - 7/2$). Interestingly, in our study all mesoporous matrices modified with vanadium and antimony give rise to well resolved signals in the hyperfine

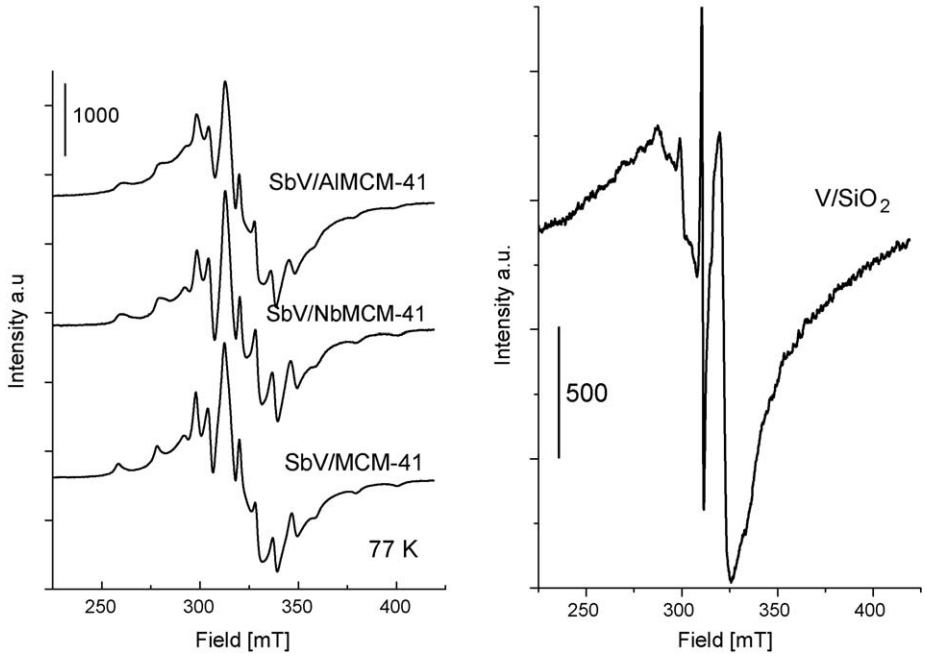

Fig. 4. ESR spectra recorded at 77 K.

Table 2
ESR results for selected samples – spectroscopic splitting tensor *g* and hyperfine structure tensor *A*.

Catalyst	$g_{\|\|}$	$A_{\|\|}$ (G)
SbV/AlMCM-41	1.935	199.4
SbV/NbMCM-41	1.933	201.2
V/NbMCM-41	1.935	202.1

Table 3
Maximum conversion of methanol (MeOH) in the reaction between hydrogen sulphide and MeOH at 623 K and selectivity for 35% conversion of methanol.

Catalyst	Maximum of MeOH conv. (%)	MeSH sel. (%)	CS_2 sel. (%)	Me_2O sel. (%)
AlMCM-41	48	16	16	68
SbV/AlMCM-41	48	51	7	42
NbMCM-41	35	97	0	3
SbV/NbMCM-41	60	98	2	0

structure of ESR spectra with *g* and *A* values characteristic for isolated VO^{2+} species (Fig. 3 and Table 2). Such a structure was not registered in the case of V/SiO_2 sample suggesting that mesoporous support is important for the isolation of oxovanadium species. Moreover, it is important to notice that bulk compounds with a rutile structure ($Sb_{0.92}{}^{5+}V_{0.8}{}^{4+}V_{0.1}{}^{3+}{}_{\cdot 0.2}O_4$) and near stoichiometric $Sb^{5+}V^{4+}O_{4.5}$ as well as $SbVO_5$ exhibit also the presence of isolated VO^{2+} ions besides dimeric species [25,26].

Various binary oxide species on the surfaces determines various catalytic activity. As concerns acidity, the Lewis acid sites (LAS) and BrØnsted acid centres (BAS) were estimated basing on FT-IR spectra after pyridine adsorption at 373 K and desorption at various temperatures. The interaction of pyridine with Lewis acid sites leads to appearing the bands at ~ 1450 and 1610 cm^{-1} [27,28]. The intensity of the first one is related to the number of LAS whereas the position of the second band characterises the strength of LAS. Adsorption of pyridine on Brønsted acid sites gives a band at 1550 cm^{-1} and two others in the 1620–1640 cm^{-1} range. Moreover, the bands at ~1445 and 1596 cm^{-1} origin from pyridine hydrogen bonded to surface hydroxyls [29]. It is clear from the examples of FT-IR spectra shown in Fig. 5 that the band at ca 1445 cm^{-1} covers both species, pyridine chemisorbed on Lewis acid sites (additional band at ca 1610 cm^{-1}) and pyridine hydrogen bonded to hydroxyls (additional band at 1596 cm^{-1}). Therefore, the band at ~1445 cm^{-1} cannot be used for the calculation of the number of Lewis acid sites. However, it is clear that impregnation of the mesoporous supports with vanadium and antimony reduces the intensity of the band due to hydrogen bonded pyridine on the surface of pristine supports. It stresses the role of surface hydroxyls in the anchoring of metal oxide species. The important finding from the FT-IR studies is that the intensity of the band assigned to pyridine bonded to Lewis acid centres increases after $SbVO_x$ loading. Moreover, BrØnsted acidity is present only on AlMCM-41 support and it is diminished after $SbVO_x$ loading. The number of BrØnsted acid centres calculated after desorption at 473 K [27] is given in Table 1.

BrØnsted acidity of the AlMCM-41 pristine sample has an important impact on the selectivity in the hydrosulphurisation of methanol with hydrogen sulphide (Table 3). This test reaction [30] clearly indicates the presence of pairs (Lewis acid and basic sites) when methanethiol (MeSH) and/or dimethyl sulphide (Me_2S) are formed. The domination of acidity or the presence of BrØnsted acid centres is demonstrated by the formation of dimethyl ether (Me_2O). The results shown in Table 3 (selectivity estimated for the same methanol conversion, i.e. 35%) well correlate with those obtained by pyridine adsorption followed by FT-IR study. AlMCM-41 sample exhibiting BrØnsted acidity is selective mainly towards dimethyl ether. This selectivity changes totally after $SbVO_x$ loading giving rise to the significantly increase of MeSH formation caused by the presence of Lewis acid–base pairs. NbMCM-41 support itself is highly selective towards MeSH (97% selectivity). However, the $SbVO_x$ loading significantly increases the maximum activity of the material (from 35 to 60%) keeping the same selectivity to MeSH. It indicates the enhancement of the amount of Lewis acid–base pairs responsible for this reaction. Bulk $SbVO_x$ samples ($SbVO_5$; $Sb_{0.92}{}^{5+}V_{0.8}{}^{4+}V_{0.1}{}^{3+}{}_{\cdot 0.2}O_4$ and $Sb^{5+}V^{4+}O_{4.5}$) described in [22,25,26,31] mixed with silica (1:3 wt. ratio) were also examined in this reaction. Their activity was very low (see

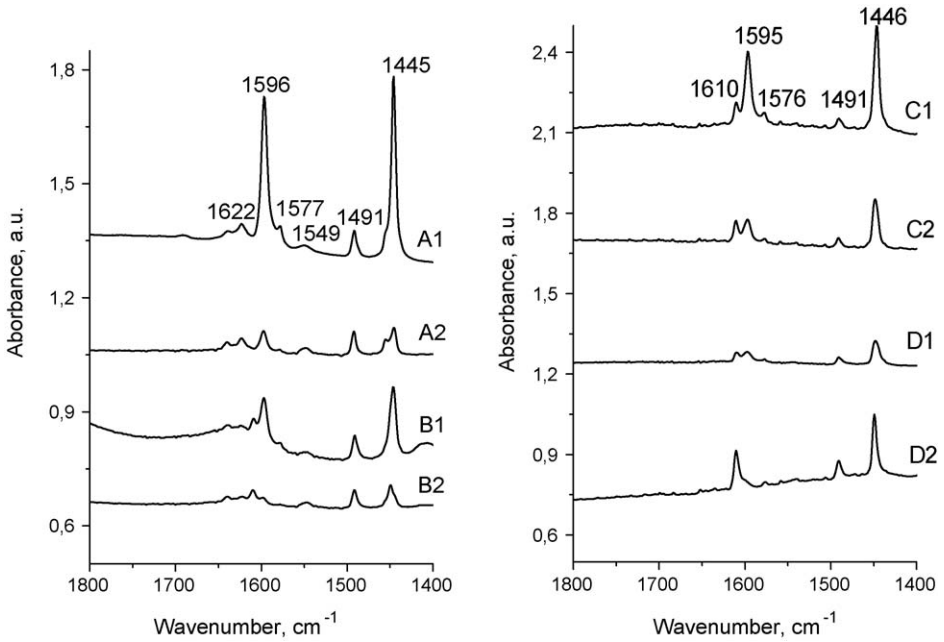

Fig. 5. FT-IR spectra after pyridine adsorption at 373 K followed by desorption at 373 K for 5 min (index 1) and 30 min (index 2) on AlMCM-41 (A): SbV/AlMCM-41 (B); NbMCM-41 (C); SbV/NbMCM-41 (D).

Table 4
Maximum conversion of methanol (MeOH) and selectivity in the reaction between hydrogen sulphide and MeOH at 623 K.

Catalyst	Maximum of MeOH conv. (%)	MeSH sel. (%)	CS_2 sel. (%)	Me_2O sel. (%)
SbV/MCM-41	18	92	6	2
$SbVO_5 + SiO_2$	4	79	21	0
$Sb_{0.92}{}^{5+}V_{0.8}{}^{4+}V_{0.1}{}^{3+}{}_{\cdot 0.2}O_4 + SiO_2$	4.5	67	33	0
$Sb^{5+}V^{4+}O^{4.5} + SiO_2$	1.8	58	42	0

Table 4), much lower than SbV/MCM-41 catalyst. This behaviour indicates the role of mesoporous support for binary $SbVO_x$ oxide in the catalytic activity. Interestingly, the catalysts presented in Table 4 are partially active towards CS_2 formation suggesting the redox behaviour of these catalysts.

4. Conclusions

Surface hydroxyls on mesoporous MCM-41 type materials play a crucial role in the anchoring of $SbVO_x$ binary oxides which are stronger hold on MCM-41 than on amorphous silica. The chemical composition of mesoporous molecular sieves determines the strength of binary oxide - support interaction and affects the dispersion, metal coordination, and isolation of metallic oxides. Tetrahedrally coordinated vanadium(IV) species were deduced from UV–vis spectra on all prepared samples. They were the only registered species on SbV/NbMCM-41 and SbV/AlMCM-41, whereas on SbV/MCM-41 and SbV/SiO_2 octahedrally ones were also present besides them. Octahedral coordination dominated in bulk $SbVO_x$.

Acid–base properties of the prepared materials are conditional on the nature of the support. BrØnsted acidity of AlMCM-41 was diminished by $SbVO_x$ loading and Lewis acid-base character of SbV/AlMCM-41 was demonstrated by high selectivity in thiol formation during the hydrosulphurisation of methanol. Lewis acid–base properties of pristine NbMCM-41 were significantly enhanced by $SbVO_x$ loading giving rise to the increase of activity in thiol formation. $SbVO_x$ supported on non active silicate MCM-41 exhibited also Lewis acid–base properties but the catalytic activity was much lower. Interestingly, the activity in hydrosulphurisation of methanol of bulk $SbVO_x$ mixed with silica was very low and selectivity significantly differed from that observed for $SbVO_x$ supported on mesoporous materials. The described results indicate the significant difference in the surface properties of $SbVO_x$ catalysts depending on the nature of mesoporous supports and the difference in catalytic activity and selectivity between bulk and supported binary oxides.

Acknowledgement

COST action D36, WG No. D36/0006/06 and the Polish Ministry of Science (Grant No. 118/COS/2007/03) are acknowledged for the financial support.

References

[1] R.K. Grasselli, Catal. Today 49 (1999) 141.
[2] S. Larrondo, B. Irigoyen, G. Baronetti, N. Amadeo, Appl. Catal. A 250 (2003) 279.
[3] G. Centi, S. Perathoner, F. Trifiro, Appl. Catal. A 157 (1997).
[4] M.O. Guerrero-Perez, M.A. Banares, Catal. Today 96 (2004) 265.
[5] M.O. Guerrero-Perez, J.L.G. Fierro, M.A. Banares, Top. Catal. 41 (2006) 43.
[6] M.O. Guerrero-Perez, J.L.G. Fierro, M.A. Banares, Catal. Today 78 (2003) 387.
[7] R. Nilsson, T. Lindblad, A. Andersson, J. Catal. 148 (1994) 501.
[8] K.M. Reddy, I. Moudrakovski, A. Sayari, J. Chem. Soc., Chem. Commun. (1994) 1059.
[9] W. Zhang, T.J. Pinnavaia, Catal. Lett. 38 (1996) 261.
[11] W. Zhang, J. Wang, P.T. Tanev, T.J. Pinnavaia, Chem. Commun. (1996) 979.
[12] W.A. Carvalho, P.B. Varaldo, M. Wallau, U. Schuchardt, Zeolites 18 (1997) 408.
[13] S. Gontier, A. Tuel, Microporous Mater. 5 (1995) 161.
[14] Z. Luan, J. Xu, H. He, J. Klinowski, L. Kevan, J. Phys. Chem. 100 (1996) 19595.
[15] K.J. Chao, C.N. Wu, H. Chang, L.J. Lee, Shu-fen Hu, J. Phys. Chem. B 101 (1997) 6341.
[16] M. Chatterjee, T. Iwasaki, H. Hayashi, Y. Onodera, T. Ebina, T. Nagase, Chem. Mater. 11 (1999) 1368.
[17] I. Hannus, T. Toth, D. Mehn, I. Kiricsi, J. Mol. Struct. 563 (564) (2001) 279–282.
[18] M. Ziolek, I. Nowak, B. Kilos, I. Sobczak, P. Decyk, M. Trejda, J.C. Volta, J. Phys. Chem. Solids 65 (2004) 571.
[19] B. Kilos, M. Aouine, I. Nowak, M. Ziolek, J.C. Volta, J. Catal. 224 (2004) 314–325.
[20] B. Kilos, J.C. Volta, I. Nowak, P. Decyk, M. Ziolek, Stud. Surf. Sci. Catal. 154 (2004) 848.
[21] B. Kilos, I. Nowak, M. Ziolek, A. Tuel, J.C. Volta, Stud. Surf. Sci. Catal. 158 (2005) 1461.
[22] E. Filipek, J. Therm. Anal. Calorim. 56 (1999) 159.
[23] C.T. Kresge, M.E. Leonowicz, W.J. Roth, J.C. Vartuli, J.S. Beck, Nature 359 (1992) 710.
[24] M. Ziolek, I. Nowak, Zeolites 18 (1997) 356.
[25] J. Typek, E. Filipek, M. Maryniak, N. Guskos, Mater. Sci.-Poland 23 (2005) 1047.
[26] J. Typek, N. Guskos, D. Buchowski, M. Wabia, E. Filipek, Radiat Eff. Defects Solids 157 (2002) 1093.
[27] S. Khabtou, T. Chevreau, J.C. Lavalley, Microporous Mater. 3 (1994) 133.
[28] E.P. Parry, J. Catal. 2 (1963) 371.
[29] B. Chakraborty, B. Viswanathan, Catal. Today 49 (1999) 253.
[30] M. Trejda, J. Kujawa, M. Ziolek, Catal. Lett. 108 (2006) 141.
[31] T. Gron, A. Krajewski, H. Duda, E. Filipek, J. Mater. Sci. 40 (2005) 5299.